Magnetic domain formation in ultrathin complex oxide ferromagnetic/antiferromagnetic bilayers

A. D. Bang,[1,a)] F. K. Olsen,[1] S. D. Slöetjes,[1,2] A. Scholl,[2] S. T. Retterer,[3] C. A. F. Vaz,[4] T. Tybell,[1] E. Folven,[1] and J. K. Grepstad[1]
[1]*Department of Electronic Systems, Norwegian University of Science and Technology (NTNU), Trondheim 7491, Norway*
[2]*Advanced Light Source, Lawrence Berkeley National Laboratory, Berkeley, California 94720, USA*
[3]*Oak Ridge National Laboratory, Oak Ridge, Tennessee 37831, USA*
[4]*Swiss Light Source, Paul Scherrer Institut, 5232 Villigen PSI, Switzerland*

(Received 6 July 2018; accepted 5 September 2018; published online 26 September 2018)

In this study, we report on the magnetic domain formation in ultrathin blanket films and patterned micro- and nanostructures of ferromagnetic (FM) $La_{0.7}Sr_{0.3}MnO_3$ single-layers and antiferromagnetic (AF)/ferromagnetic $LaFeO_3/La_{0.7}Sr_{0.3}MnO_3$ bilayers, as investigated by soft x-ray photoemission electron microscopy. In single-layer $La_{0.7}Sr_{0.3}MnO_3$, the domain size is significantly reduced compared to that found in thicker layers, and rectangular micromagnets display metastable multidomain states distinctly different from the flux-closure ground states commonly found in thicker elements. In the $LaFeO_3/La_{0.7}Sr_{0.3}MnO_3$ bilayers, complex multidomain patterns are observed for blanket films and patterned magnets with robust perpendicular (spin-flop) coupling between spins in the AF and FM layers. By thermal cycling of the sample through the $La_{0.7}Sr_{0.3}MnO_3$ Curie temperature, we find that the native antiferromagnetic domain pattern of $LaFeO_3$ pins the location of domain boundaries in the adjacent $La_{0.7}Sr_{0.3}MnO_3$ layer. *Published by AIP Publishing.*
https://doi.org/10.1063/1.5047271

Complex oxide heterostructures are promising for device applications due to their wide range of functional properties. Their interfaces attract special attention, with novel physical properties emerging from structural, electronic, and orbital reconstructions.[1–3] However, a pronounced dependence of the order parameters on the layer thicknesses has been reported for ultrathin layers,[4–7] which is likely to affect the interface coupling and thus the functional properties. Exploring how critical length scales impact these properties is paramount for successful implementation in functional devices.

When grown epitaxially on (001)-oriented $SrTiO_3$ substrates, thin film bilayers of antiferromagnetic (AF) $LaFeO_3$ (LFO) with a fully compensated surface of Fe^{3+} moments and ferromagnetic (FM) $La_{0.7}Sr_{0.3}MnO_3$ (LSMO) have been shown to exhibit perpendicular spin alignment across the interface, i.e., spin-flop coupling.[8,9] In addition, by relying on a shape-induced domain formation in the antiferromagnet, it is possible to engineer a collinear spin alignment in micro- and nanomagnets[10] and tune the switching field for patterned LFO/LSMO bilayer magnets.[11,12]

In this letter, we show how the magnetic domain pattern is modified in LSMO blanket films and LFO/LSMO bilayers when the FM layer thickness is reduced to a value near that of the reported "dead layer" in manganite thin films.[13–15] In bilayer micro- and nanomagnets, we invariably observe a close correlation between the AF and FM domains, with a robust spin-flop coupling. Measurements carried out above and below the LSMO Curie temperature (T_c) indicate that the domain pattern is formed in competition between the native AF domain structure of the LFO layer and magnetic anisotropies in the LSMO layer.

The single-layer LSMO and bilayer LFO/LSMO thin films were grown by pulsed laser deposition on (001)-oriented, Nb-doped (0.05 wt. %) $SrTiO_3$ substrates. The FM layer was grown with a thickness of either 100, 20, or 10 unit cells (u.c.) (1 u.c. ≈ 0.4 nm), whereas the AF top layer in all bilayer samples was 10 u.c. Epitaxial growth was achieved using growth conditions reported elsewhere.[16,17] Rectangular nano- and microstructures of different lateral dimensions were defined using Ar^+-ion implantation through a Cr hard mask or a resist (CSAR69) soft mask defined by electron beam lithography. Where not protected by this mask, the Ar^+ ions penetrate the full film thickness, disrupting the magnetic order in the ferro- and antiferromagnetic layers alike. Subsequent removal of the implantation mask leaves an array of magnets embedded in a paramagnetic matrix. This structuring technique is discussed in detail in earlier publications.[10,16,18,19]

Images of the magnetic domain structure formed spontaneously in blanket films (as grown) and after patterning (micromagnets) were recorded by soft x-ray spectromicroscopy, using the photoemission electron microscope (PEEM-3) at the Advanced Light Source (ALS) and the Surface/Interface Microscopy beamline (SIM) at the Swiss Light Source (SLS). The FM domain contrast was obtained from magnetic circular dichroism (XMCD) at the Mn L_3 absorption edge and the AF domain contrast from magnetic linear dichroism (XMLD) in the absorption of s-polarized x-rays at photon energies corresponding to the two maxima of the Fe L_2 multiplet. Restricting the film thickness of the top AF layer to 10 u.c. allows imaging of the magnetic order in the individual layers of the LFO/LSMO bilayer films.

a)Author to whom correspondence should be addressed: ambjorn.bang@ntnu.no

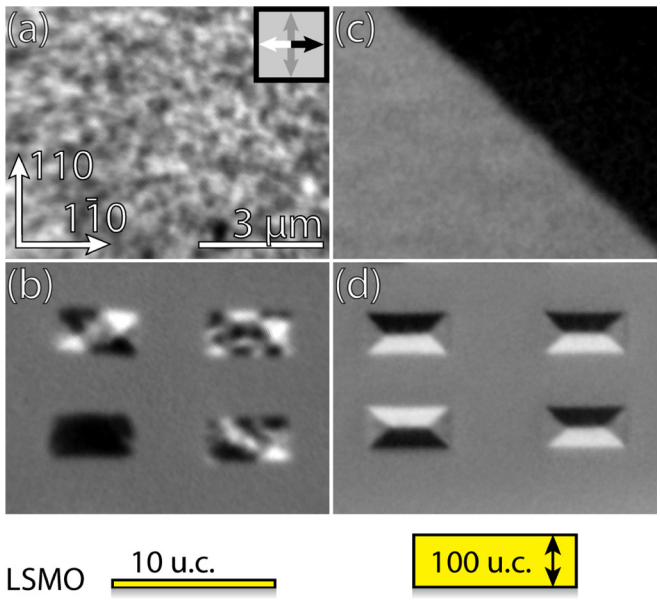

FIG. 1. XMCD-PEEM images of ferromagnetic domain patterns recorded for an ultrathin (10 u.c.) and a thick (100 u.c.) LSMO thin film. (a) and (b) show magnetic domain contrast for a 10 u.c. blanket film and 2×1 μm^2 rectangular micromagnets, respectively. (c) and (d) show the equivalent domain patterns for a 100 u.c. LSMO thin film. The correspondence between the X-PEEM domain contrast and the direction of magnetization of individual domains is seen from the legend in (a).

Figure 1 shows X-PEEM images comparing magnetic domain patterns characteristic of the 10 u.c. LSMO blanket film (a) and 2×1 μm^2 micromagnets (b) patterned on the same sample with those recorded for a 100 u.c. blanket film (c) and the corresponding micromagnets (d). In the 10 u.c. blanket film, we observe a speckled FM domain pattern with a typical domain size on the order of ~100 nm [Fig. 1(a)]. This domain pattern differs considerably from that observed for a thicker LSMO layer, which typically displays magnetic domains with several μm lateral dimensions [Fig. 1(c)], with their moments oriented along the magnetocrystalline easy directions (i.e., the in-plane ⟨110⟩ directions).[20–22] For the 2×1 μm^2 rectangular magnets defined in the 10 u.c. film [Fig. 1(b)], most structures were found to be either monodomain or display a multidomain pattern reminiscent of that seen in the blanket film, with only a few showing the characteristic flux-closure domain patterns invariably observed for magnets defined in thicker films [Fig. 1(d), cf. also Refs. 18 and 23]. The loss of flux-closure domain states in the rectangular micromagnets and the distinct transformation of the domain pattern in blanket films when the LSMO film thickness is reduced to 10 u.c. suggest a shift in the balance between magnetostatic and domain wall energies. The smaller magnetic volume of the 10 u.c. LSMO layer implies a lower driving force towards flux-closure patterns, rendering the film prone to metastable domain states different from the FM ground state observed in thicker films.[18,23] We note that Heyderman *et al.* have reported similar results for ultrathin polycrystalline permalloy and cobalt thin film microstructures.[24]

The impact of the FM layer thickness on the magnetic domain formation in ultrathin bilayer films is displayed in Fig. 2. In the 10/20 u.c. LFO/LSMO blanket film, the LSMO layer forms micrometer-sized FM domains magnetized along in-plane ⟨110⟩ directions [Fig. 2(a)]. Rectangular structures

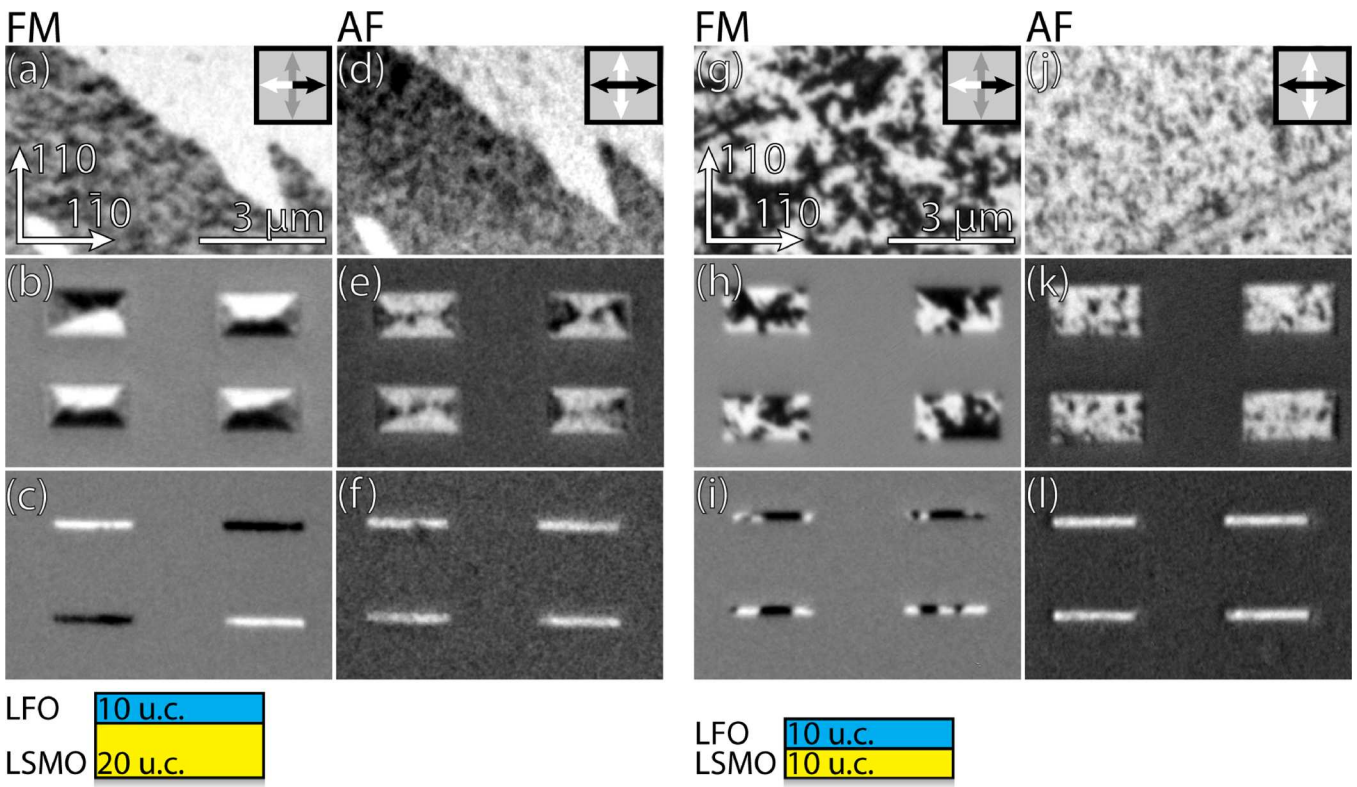

FIG. 2. XMCD- and XMLD-PEEM images showing the FM and AF domain patterns of 10/20 u.c. (a)–(f) and 10/10 u.c. (g)–(l) LFO/LSMO bilayer samples at $T < T_C$ ($T = 100$ K). Images in (a), (d), (g), and (j) show the domain pattern for blanket films; (b), (e), (h), and (k) the domain patterns for 1×2 μm^2 rectangles; and (c), (f), (i), and (l) the domain patterns for 200 nm × 2 μm line segments. Legends showing the correspondence between X-PEEM domain contrast and direction of magnetization apply for all three images in each column.

with their edges aligned along these axes display domain patterns dictated by shape anisotropy, i.e., a flux-closure pattern for $1 \times 2\ \mu m^2$ rectangles [Fig. 2(b)] and uniformly magnetized (monodomain) $200\,nm \times 2\,\mu m$ line segments [Fig. 2(c)]. The corresponding AF domain patterns, shown in Figs. 2(d)–2(f), are all consistent with spin-flop coupling to the underlying FM layer and thus agree with the behavior previously reported for LFO/LSMO heterostructures with a thicker LSMO layer.[8,9] We note that the large domains in the blanket film are speckled with minor domains of a different contrast, and the flux-closure domain states of the rectangular magnets are noticeably distorted compared to those reported for magnets defined in a bilayer film with a thicker FM layer.[9] The latter observation suggests an increased impact from the antiferromagnet on the FM domain formation in the 10/20 u.c. sample.

The bilayer sample with a thinner (10 u.c.) FM layer displays a pronounced shift in the magnetic domain pattern from that of the 10/20 u.c. sample. The blanket film FM domains [Fig. 2(g)] are orders-of-magnitude smaller and bear a close resemblance to the domain pattern commonly observed for an AF blanket film.[25,26] The patterned structures exhibit no apparent FM domain formation driven by shape anisotropy [Figs. 2(h) and 2(i)]. The corresponding AF domain patterns [Figs. 2(k) and 2(l)] confirm a persistent spin-flop coupling, domain-by-domain, also in these ultrathin LFO/LSMO bilayer samples.

Figures 3(a)–3(e) show the recorded domain pattern for a $2 \times 1\ \mu m^2$ 10/10 u.c. bilayer micromagnet at three different temperatures; $T = 250\,K$ (well above $T_C \sim 200\,K$ for this ultrathin LSMO layer), $T = 195\,K$ (right below T_C), and $T = 150\,K$ (well below T_C). The AF domain pattern at $T = 250\,K$ [Fig. 3(a)] displays extended domains along the micromagnet edges with the AF spin axis aligned parallel to those the edges, consistent with the shape-imposed alignment previously reported for structures defined in LFO single-layer films[10] and LFO/LSMO bilayers for $T > T_C$.[16] Figures 3(b) and 3(c) show the XMCD- and XMLD-PEEM images taken at $T = 195\,K$, the maximum temperature at which FM domain contrast could be obtained for this sample. While the AF domain pattern remains unchanged at this temperature, the FM domains in the LSMO layer now closely match the AF domain pattern with perpendicular (spin-flop) coupling of the AF spins and the FM moments. These data suggest a magnetic domain formation governed by the AF (LFO) layer. A similar FM/AF domain coupling was previously reported by Nolting *et al.*[27] for an ultrathin (1.2 nm) layer of Co deposited on a 40 nm thick film of LFO. Upon further reduction of the temperature to $T = 150\,K$ [Figs. 3(d) and 3(e)], a spin reorientation is found both in the AF and FM layers. However, spin-flop coupling between the two layers persists domain by domain. No further domain reconfiguration was observed for temperatures down to $T = 100\,K$.

With a T_C estimated at $\sim$200 K from the XMCD data, the saturation magnetization increases significantly when the sample temperature is lowered from 195 K to 150 K (from zero to $\sim$60 % of the saturation magnetization at $T = 100\,0\,K$ for a 10/10 u.c. LFO/LSMO blanket film, estimated from magnetometry measurements not shown), whereas we expect little variation of the AF order parameter

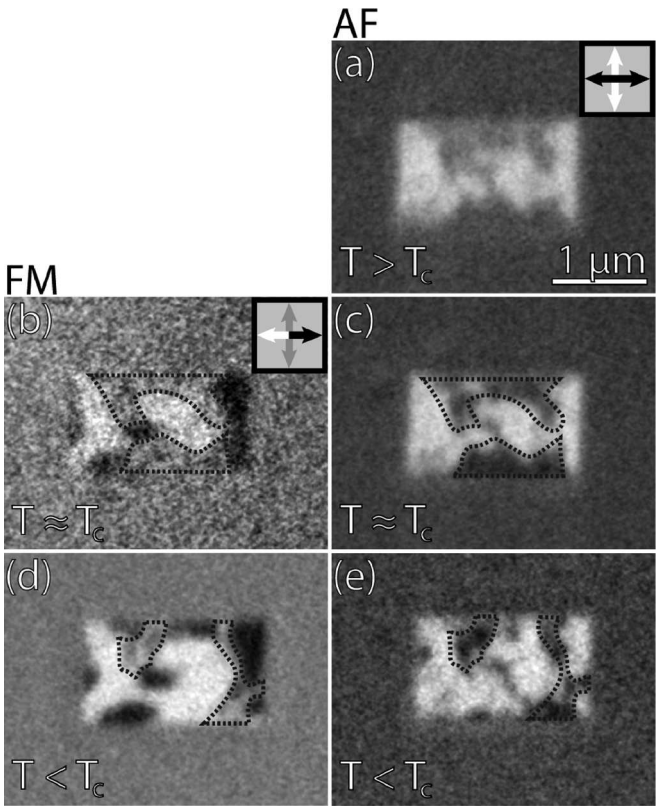

FIG. 3. XMCD- and XMLD-PEEM images showing characteristic magnetic domain patterns at different temperatures; (a) $T = 250\,K$, (b) and (c) $T = 195\,K$, and (d) and (e) $T = 150\,K$ for a $1 \times 2\ \mu m^2$ rectangle defined in an LFO/LSMO bilayer film. Grey domains in the FM domain images and corresponding regions in the AF domain images are outlined for clarity.

in this temperature interval, assuming a Néel temperature (T_N) of $\sim$640 K for the thin LFO layer.[25,28] Increased magnetization in the FM layer promotes the formation of domains, effectively minimizing the demagnetization energy.[18,23] The absence of flux-closure domain patterns in the 10/10 u.c. bilayer micromagnets indicates that the magnetostatic energies in the FM layer are insufficient to overcome the interface exchange coupling to the adjacent antiferromagnet in this sample.

The observed reorientation of FM moments and AF spins in the temperature range of 150–195 K is most prominent for domains located along the edges of the rectangular micromagnets. Both the FM shape anisotropy and the previously reported shape effects in the antiferromagnet favor alignment of the magnetic moments parallel to the micromagnet edges.[10] However, such spin alignment in both layers is not compatible with spin-flop coupling. Close to T_C, the FM demagnetization energy is insufficient to overcome the spin-flop coupling and force the FM moments to line up along the edges, leading to FM domains with their magnetization oriented perpendicular to the edges. Likewise, the reorientation of FM and AF spins observed at lower temperatures results in a predominance of domains with FM moments aligned parallel to the micromagnet edges with a perpendicular orientation of the AF spins. Certain edge domains were found to retain the orientation of the FM spins perpendicular to the micromagnet edges at low temperature. In these domains, the FM shape anisotropy is insufficient to

override the shape effects in the antiferromagnet and induce a rotation of the AF spins, creating a "frustrated" domain pattern. This observation is a clear indication of the robust spin-flop coupling in these ultrathin AF/FM bilayers. A similar spin-flop coupling of FM and AF domains was previously reported by Yang *et al.*[29] for a blanket film LSMO/$La_{0.7}Sr_{0.3}FeO_3$ (LSFO) $[6\text{ u.c.} \times 6\text{ u.c.}]_{10}$ superlattice, where the AF spin axis was shown to reorient in response to the application of an in-plane magnetic field.

Figure 4 displays X-PEEM images recorded upon repeated thermal cycling through T_C of the 10/10 u.c. LFO/LSMO micromagnet shown in Fig. 3. The AF domain pattern recorded above T_C [Figs. 4(a)–4(c)] remains unaffected by this thermal cycling, presumably pinned by structural domains which typically define the AF domains in thin LFO films.[26,30] In the measurements taken at $T = 150\text{ K}$ [Figs. 4(d)–4(i)], we note distinct changes to the AF and FM domain patterns. However, spin-flop coupling is invariably preserved within individual domains.

While spin reorientation is frequently found upon thermal cycling, the domain walls of the spin-flop coupled domains tend to remain fixed at the domain boundaries of the high temperature ($T > T_C$) AF domain pattern. This observation suggests that the interface-coupled AF/FM domain patterns below T_C are seeded by the native AF domain structure. At low temperature, the magnetostatic energy of the FM layer thus appears to be sufficient for reorientation of the FM moments within individual domains with a concurrent rotation of the AF spin axis to comply with spin-flop coupling, but insufficient to disrupt the domain boundaries pinned by the LFO thin film microstructure.

In summary, we have investigated the magnetic domain formation in FM LSMO thin films and AF/FM LFO/LSMO bilayers, where the thickness of the LSMO layer approaches the reported limit of bulk-like magnetic behavior.[15] We find that an ultrathin layer thickness of 10 u.c. (~4 nm) profoundly affects the FM domain pattern with loss of the large FM domains found in thicker films.[20–22] Moreover, the flux-closure ground state commonly observed for square/rectangular micromagnets defined in films with thicker LSMO layer[18,23] is replaced by metastable multidomain states. The reduced magnetostatic energy of the 10 u.c. LSMO single-layer and the 10/10 u.c. LFO/LSMO bilayer leads to magnetic domain patterns significantly different from those recorded for bilayer magnets with a thicker FM layer.[9] At low temperature, the magnetostatic energy is sufficient for the local reorientation of FM moments with a concomitant rotation of the AF spin axis driven by a robust spin-flop coupling. However, the FM domain boundaries remain fixed, seeded by the AF domain structure of the LFO layer above T_C. These findings shed light on the domain formation in ultrathin oxide thin film micro-/nanomagnets, which may prove essential to the use of magnetic oxide heterostructures for device applications.

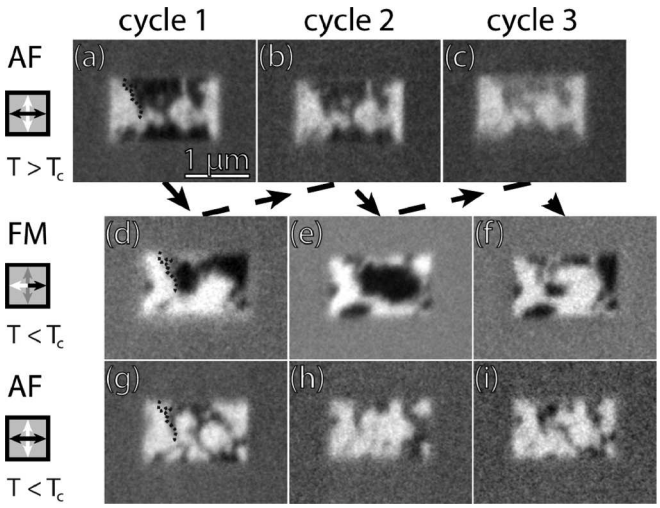

FIG. 4. XMCD- and XMLD-PEEM images showing three thermal cycles of a 10/10 u.c. bilayer structure: (a) and (b) recorded at $T = 200\text{ K}$ and (c) recorded at $T = 250\text{ K}$; all showing the AF domain pattern for $T > T_C$. (d)–(f) The FM domain pattern and (g)–(i) the AF domain pattern recorded at $T = 150\text{ K}$. The dashed arrows indicate the timeline of the measurements with thermal cycling. In (a), an AF domain boundary has been outlined for clarity. This domain boundary is traced in (d) and (g) to emphasize the preservation of the AF domain boundaries through the first temperature cycle.

This research was undertaken with financial support from the Research Council of Norway under Grant No. 231290. Funding was also obtained from the Norwegian PhD Network on Nanotechnology for Microsystems (A.D.B.), which is sponsored by the Research Council of Norway, Division for Science, under Contract No. 221860/F60. X-PEEM measurements were carried out in part on beamline 11.0.1.1, the Advanced Light Source, Lawrence Berkeley National Laboratory, and in part on the SIM beamline, the Swiss Light Source, Paul Scherrer Institute, Villigen. The Advanced Light Source is supported by the Director, Office of Science, Office of Basic Energy Sciences, and the U.S. Department of Energy under Contract No. DE-AC02-05CH11231. Nanoscale patterning was carried out at the Center for Nanophase Materials Sciences, which is a U.S. DOE Office of Science User Facility.

[1]H. Y. Hwang, Y. Iwasa, M. Kawasaki, B. Keimer, N. Nagaosa, and Y. Tokura, Nat. Mater. **11**, 103 (2012).
[2]J. Chakhalian, A. J. Millis, and J. Rondinelli, Nat. Mater. **11**, 92 (2012).
[3]C. A. F. Vaz, F. J. Walker, C. H. Ahn, and S. Ismail-Beigi, J. Phys.: Condens. Matter **27**(12), 123001 (2015).
[4]J. Junquera and P. Ghosez, Nature **422**, 506 (2003).
[5]J. Z. Sun, D. W. Abraham, R. A. Rao, and C. B. Eom, Appl. Phys. Lett. **74**(20), 3017 (1999).
[6]R. Scherwitzl, S. Gariglio, M. Gabay, P. Zubko, M. Gibert, and J.-M. Triscone, Phys. Rev. Lett. **106**(24), 246403 (2011).
[7]J. Y. Zhang, C. A. Jackson, S. Raghavan, J. Hwang, and S. Stemmer, Phys. Rev. B **88**(12), 121104 (2013).
[8]E. Folven, A. Scholl, A. Young, S. T. Retterer, J. E. Boschker, T. Tybell, Y. Takamura, and J. K. Grepstad, Nano Lett. **12**(5), 2386 (2012).
[9]Y. Takamura, E. Folven, J. B. R. Shu, K. R. Lukes, B. Li, A. Scholl, A. T. Young, S. T. Retterer, T. Tybell, and J. K. Grepstad, Phys. Rev. Lett. **111**(10), 107201 (2013).
[10]E. Folven, T. Tybell, A. Scholl, A. Young, S. T. Retterer, Y. Takamura, and J. K. Grepstad, Nano Lett. **10**(11), 4578 (2010).
[11]E. Folven, J. Linder, O. V. Gomonay, A. Scholl, A. Doran, A. T. Young, S. T. Retterer, V. K. Malik, T. Tybell, Y. Takamura, and J. K. Grepstad, Phys. Rev. B **92**(9), 094421 (2015).
[12]M. S. Lee, T. A. Wynn, E. Folven, R. V. Chopdekar, A. Scholl, S. T. Retterer, J. K. Grepstad, and Y. Takamura, Phys. Rev. Mater. **1**(1), 014402 (2017).
[13]J. J. Kavich, M. P. Warusawithana, J. W. Freeland, P. Ryan, X. Zhai, R. H. Kodama, and J. N. Eckstein, Phys. Rev. B **76**(1), 014410 (2007).

[14]M. Huijben, L. W. Martin, Y. H. Chu, M. B. Holcomb, P. Yu, G. Rijnders, D. H. A. Blank, and R. Ramesh, Phys. Rev. B **78**(9), 094413 (2008).
[15]Å. F. Monsen, J. E. Boschker, F. Macià, J. W. Wells, P. Nordblad, A. D. Kent, R. Mathieu, T. Tybell, and E. Wahlström, J. Magn. Magn. Mater. **369**, 197 (2014).
[16]E. Folven, A. Scholl, A. Young, S. T. Retterer, J. E. Boschker, T. Tybell, Y. Takamura, and J. K. Grepstad, Phys. Rev. B **84**(22), 220410 (2011).
[17]J. E. Boschker, E. Folven, Å. F. Monsen, E. Wahlström, J. K. Grepstad, and T. Tybell, Cryst. Growth Des. **12**(2), 562 (2012).
[18]Y. Takamura, R. V. Chopdekar, A. Scholl, A. Doran, J. A. Liddle, B. Harteneck, and Y. Suzuki, Nano Lett. **6**(6), 1287 (2006).
[19]E. Folven, Y. Takamura, and J. K. Grepstad, J. Electron Spectrosc. Relat. Phenom. **185**(10), 381 (2012).
[20]P. Lecoeur, P. L. Trouilloud, G. Xiao, A. Gupta, G. Q. Gong, and X. W. Li, J. Appl. Phys. **82**(8), 3934 (1997).
[21]T. Taniuchi, R. Yasuhara, H. Kumigashira, M. Kubota, H. Okazaki, T. Wakita, T. Yokoya, K. Ono, M. Oshima, M. Lippmaa, M. Kawasaki, and H. Koinuma, Surf. Sci. **601**(20), 4690 (2007).
[22]R. M. Reeve, C. Mix, M. König, M. Foerster, G. Jakob, and M. Kläui, Appl. Phys. Lett. **102**(12), 122407 (2013).
[23]M. S. Lee, T. A. Wynn, E. Folven, R. V. Chopdekar, A. Scholl, A. T. Young, S. T. Retterer, J. K. Grepstad, and Y. Takamura, ACS Nano **10**(9), 8545 (2016).
[24]L. J. Heyderman, S. Czekaj, F. Nolting, E. Müller, P. Fischer, P. Gasser, and L. López-Díaz, J. Appl. Phys. **99**(6), 063904 (2006).
[25]A. Scholl, J. Stöhr, J. Lüning, J. W. Seo, J. Fompeyrine, H. Siegwart, J.-P. Locquet, F. Nolting, S. Anders, E. E. Fullerton, M. R. Scheinfein, and H. A. Padmore, Science **287**(5455), 1014 (2000).
[26]S. Czekaj, F. Nolting, L. J. Heyderman, K. Kunze, and M. Krüger, J. Phys.: Condens. Matter **19**(38), 386214 (2007).
[27]F. Nolting, A. Scholl, J. Stohr, J. W. Seo, J. Fompeyrine, H. Siegwart, J.-P. Locquet, S. Anders, J. Luning, E. E. Fullerton, M. F. Toney, M. R. Scheinfein, and H. A. Padmore, Nature **405**(6788), 767 (2000).
[28]J. K. Grepstad, Y. Takamura, A. Scholl, I. Hole, Y. Suzuki, and T. Tybell, Thin Solid Films **486**(1), 108 (2005).
[29]F. Yang, N. Kemik, A. Scholl, A. Doran, A. T. Young, M. D. Biegalski, H. M. Christen, and Y. Takamura, Phys. Rev. B **83**(1), 014417 (2011).
[30]I. Hallsteinsen, M. Moreau, R. V. Chopdekar, E. Christiansen, M. Nord, P. E. Vullum, J. K. Grepstad, R. Holmestad, S. M. Selbach, A. Scholl, E. Arenholz, E. Folven, and T. Tybell, APL Mater. **5**(8), 086107 (2017).